



HAL
open science

Threshold of a random laser based on Raman gain in cold atoms

William Guerin, Nicolas Mercadier, Davide Brivio, Robin Kaiser

► **To cite this version:**

William Guerin, Nicolas Mercadier, Davide Brivio, Robin Kaiser. Threshold of a random laser based on Raman gain in cold atoms. *Optics Express*, 2009, 17 (14), pp.11236. hal-00370950v2

HAL Id: hal-00370950

<https://hal.science/hal-00370950v2>

Submitted on 23 Jun 2009

HAL is a multi-disciplinary open access archive for the deposit and dissemination of scientific research documents, whether they are published or not. The documents may come from teaching and research institutions in France or abroad, or from public or private research centers.

L'archive ouverte pluridisciplinaire **HAL**, est destinée au dépôt et à la diffusion de documents scientifiques de niveau recherche, publiés ou non, émanant des établissements d'enseignement et de recherche français ou étrangers, des laboratoires publics ou privés.

Threshold of a random laser based on Raman gain in cold atoms

William Guerin, Nicolas Mercadier, Davide Brivio¹ and Robin Kaiser

*Institut Non Linéaire de Nice, CNRS and Université de Nice Sophia-Antipolis,
1361 route des Lucioles, 06560 Valbonne, France*

¹*Present address: Dipartimento di Fisica, Università di Milano, I-20113, Italy*

william.guerin@inln.cnrs.fr

<http://www.kaiserlux.de/coldatoms/>

Abstract: We address the problem of achieving a random laser with a cloud of cold atoms, in which gain and scattering are provided by the same atoms. In this system, the elastic scattering cross-section is related to the complex atomic polarizability. As a consequence, the random laser threshold is expressed as a function of this polarizability, which can be fully determined by spectroscopic measurements. We apply this idea to experimentally evaluate the threshold of a random laser based on Raman gain between non-degenerate Zeeman states and find a critical optical thickness on the order of 200, which is within reach of state-of-the-art cold-atom experiments.

© 2009 Optical Society of America

OCIS codes: (140.1340) Atomic gas lasers; (140.3550) Lasers, Raman; (290.4210) Multiple scattering

References and links

1. V. S. Letokhov, "Generation of light by a scattering medium with negative resonance absorption," *Sov. Phys. JETP* **26**, 835–840 (1968).
2. C. Gouedard, D. Husson, D. Sauteret, F. Auzel, and A. Migus, "Generation of spatially incoherent short pulses in laser-pumped neodymium stoichiometric crystals and powders," *J. Opt. Soc. Am. B* **10**, 2358–2362 (1993).
3. J. Martorell, R. M. Balachandran, and N. M. Lawandy, "Radiative coupling between photonic paint layers," *Opt. Lett.* **21**, 239–241 (1996).
4. H. Cao, Y. G. Zhao, H. C. Ong, S. T. Ho, J. Y. Dai, J. Y. Wu, and R. P. H. Chang, "Ultraviolet Lasing in Resonators Formed by Scattering in Semiconductor Polycrystalline Films," *Appl. Phys. Lett.* **73**, 3656–3658 (1998).
5. D. S. Wiersma and S. Cavalier, "Light emission: A temperature-tunable random laser," *Nature* **414**, 708–709 (2001).
6. G. Strangi, S. Ferjani, V. Barna, A. D. Luca, C. Versace, N. Scaramuzza, and R. Bartolino, "Random lasing and weak localization of light in dye-doped nematic liquid crystals," *Opt. Express* **14**, 7737–7744 (2006).
7. D. S. Wiersma and A. Lagendijk, "Light diffusion with gain and random lasers," *Phys. Rev. E* **54**, 4256–4265 (1996).
8. A. L. Burin, M. A. Ratner, H. Cao, and R. P. H. Chang, "Model for a Random Laser," *Phys. Rev. Lett.* **87**, 215503 (2001).
9. C. Vanneste, P. Sebbah, and H. Cao, "Lasing with Resonant Feedback in Weakly Scattering Random Systems," *Phys. Rev. Lett.* **98**, 143902 (2007).
10. H. E. Türeci, L. Ge, S. Rotter, and A. D. Stone, "Strong Interactions in Multimode Random Lasers," *Science* **320**, 643–646 (2008).
11. D. S. Wiersma, "The physics and applications of random lasers," *Nat. Phys.* **4**, 359–367 (2008).
12. C. Conti and A. Fratalocchi, "Dynamic light diffusion, three-dimensional Anderson localization and lasing in inverted opals," *Nat. Phys.* **4**, 794–798 (2008).

13. H. Cao, "Lasing in random media," *Waves Random Media* **13**, R1–R39 (2003).
14. H. Cao, "Review on latest developments in random lasers with coherent feedback," *J. Phys. A* **38**, 10497–10535 (2005).
15. H. Metcalf and P. van der Straten, *Laser cooling and Trapping* (Springer, New York, 1999).
16. A. Fioretti, A. F. Molisch, J. H. Mutter, P. Verkerk, and M. Allegrini, "Observation of radiation trapping in a dense Cs magneto-optical trap," *Opt. Commun.* **149**, 415–422 (1998).
17. G. Labeurie, E. Vaujour, C. A. Müller, D. Delande, C. Miniatura, D. Wilkowski, and R. Kaiser, "Slow Diffusion of Light in a Cold Atomic Cloud," *Phys. Rev. Lett.* **91**, 223904 (2003).
18. L. Hilico, C. Fabre, and E. Giacobino, "Operation of a "Cold-Atom Laser" in a Magneto-Optical Trap," *Europhys. Lett.* **18**, 685–688 (1992).
19. W. Guerin, F. Michaud, and R. Kaiser, "Mechanisms for Lasing with Cold Atoms as the Gain Medium," *Phys. Rev. Lett.* **101**, 093002 (2008).
20. Note that even though new interesting features appear when coherent feedback is involved [14], we will consider only incoherent (intensity) feedback.
21. L. S. Froufe-Pérez, W. Guerin, R. Carminati, and R. Kaiser, "Threshold of a Random Laser with Cold Atoms," *Phys. Rev. Lett.* **102**, 173903 (2009).
22. B. R. Mollow, "Stimulated Emission and Absorption near Resonance for Driven Systems," *Phys. Rev. A* **5**, 2217–2222 (1972).
23. J. D. Jackson, *Classical Electrodynamics*, 3rd ed. (Wiley, New York, 1999).
24. D. Grison, B. Lounis, C. Salomon, J.-Y. Courtois, and G. Grynberg, "Raman Spectroscopy of Cesium Atoms in a Laser Trap," *Europhys. Lett.* **15**, 149–154 (1991).
25. J. W. R. Tabosa, G. Chen, Z. Hu, R. B. Lee, and H. J. Kimble, "Nonlinear Spectroscopy of Cold Atoms in a Spontaneous-Force Optical Trap," *Phys. Rev. Lett.* **66**, 3245–3248 (1991).
26. M. C. W. van Rossum and T. M. Nieuwenhuizen, "Multiple scattering of classical waves: microscopy, mesoscopy, and diffusion," *Rev. Mod. Phys.* **71**, 313–371 (1999).
27. We consider only isotropic scattering so that the transport length equals the scattering mean free path [26].
28. K. Case and P. Zweifel, *Linear transport theory* (Addison-Wesley, 1967).
29. K. Drozdowicz, E. Krynicka, and J. Dąbrowska, "Diffusion cooling of thermal neutrons in basic rock minerals by Monte Carlo simulation of the pulsed neutron experiments," *App. Rad. Isot.* **58**, 727–733 (2003).
30. A. Legendijk and B. A. van Tiggelen, "Resonant multiple scattering of light," *Phys. Rep.* **270**, 143–215 (1996).
31. D. Brivio, "Random laser with cold atoms: extracting information from atomic fluorescence," Master Thesis, Università di Milano (2008).
32. T. M. Brzozowski, M. Brzozowska, J. Zachorowski, M. Zawada, and W. Gawlik, "Probe spectroscopy in an operating magneto-optical trap: The role of Raman transitions between discrete and continuum atomic states," *Phys. Rev. A* **71**, 013401 (2005).
33. G. Grynberg and C. Robilliard, "Cold atoms in dissipative optical lattices," *Phys. Rep.* **355**, 335–451 (2001).
34. Y.-C. Chen, Y.-W. Chen, J.-J. Su, J.-Y. Huang, and I. A. Yu, "Pump-probe spectroscopy of cold ^{87}Rb atoms in various polarization configurations," *Phys. Rev. A* **63**, 043808 (2001).
35. C. Cohen-Tannoudji, J. Dupont-Roc, and G. Grynberg, *Atom-Photon Interactions: Basic Processes and Applications* (Wiley, New York, 1992).
36. B. Gao, "Effects of Zeeman degeneracy on the steady-state properties of an atom interacting with a near-resonant laser field: Resonance fluorescence," *Phys. Rev. A* **50**, 4139–4156 (1994).
37. B. R. Mollow, "Power Spectrum of Light Scattered by Two-Level Systems," *Phys. Rev.* **188**, 1969–1975 (1969).
38. W. Ketterle, K. B. Davis, M. A. Joffe, A. Martin, and D. E. Pritchard, "High Densities of Cold Atoms in a Dark Spontaneous-Force trap," *Phys. Rev. Lett.* **70**, 2253–2256 (1993).
39. M. T. dePue, S. L. Winoto, D. J. Han, and D. S. Weiss, "Transient compression of a MOT and high intensity fluorescent imaging of optically thick clouds of atoms," *Opt. Commun.* **180**, 73–79 (2000).
40. C. I. Westbrook, R. N. Watts, C. E. Tanner, S. L. Rolston, W. D. Phillips, P. D. Lett, and P. L. Gould, "Localization of atoms in a three-dimensional standing wave," *Phys. Rev. Lett.* **65**, 33–36 (1990).
41. C. Jurczak, K. Sengstock, R. Kaiser, N. Vansteenkiste, C. I. Westbrook, and A. Aspect, "Observation of intensity correlations in the fluorescence from laser cooled atoms," *Opt. Commun.* **115**, 480–484 (1995).
42. S. Bali, D. Hoffmann, J. Simán, and T. Walker, "Measurements of intensity correlations of scattered light from laser-cooled atoms," *Phys. Rev. A* **53**, 3469–3472 (1996).
43. M. A. Noginov, J. Novak, D. Grigsby, and L. Deych, "Applicability of the diffusion model to random lasers with non-resonant feedback," *J. Opt. A: Pure Appl. Opt.* **8**, S285–S295 (2006).

1. Introduction

Random lasing occurs when the optical feedback due to multiple scattering (or "radiation trapping") in a gain medium is strong enough so that gain in the sample volume overcomes losses through the surface. Since its theoretical prediction by Letokhov [1], great efforts have been

made to experimentally demonstrate this effect in different kinds of systems [2, 3, 4, 5, 6], as well as to understand the fundamentals of random lasing [7, 8, 9, 10]. The broad interest of this topic is driven by potential applications (see [11] and references therein) and by its connections to the fascinating subject of Anderson localization [12]. State-of-the-art random lasers [11, 13, 14] are usually based on condensed matter systems, and feedback is provided by a disordered scattering medium, while gain is provided by an active material lying in the host medium or inside the scatterers. In general, scattering and gain are related to different physical entities.

Another system that can be considered for achieving random lasing is a cold atomic vapor, using magneto-optical traps [15], where radiation trapping [16, 17] as well as lasing [18, 19] have already been demonstrated. One advantage is the ability to characterize and model the microscopic properties of the medium, which can be extremely valuable for a better understanding of the physics of random lasers.

However, in such system, the ability to combine gain and multiple scattering at the same time is not obvious, as both should be provided by the same atoms. On the other hand, it has been shown recently that the peculiarity of this system leads to a simple condition for random lasing in the incoherent regime [20]. The threshold is indeed defined as a critical on-resonance optical thickness b_0 , which is a function of the complex atomic polarizability α as the single parameter [21]. This has been used to predict theoretically the threshold of a random laser based on Mollow gain, for which the atomic polarizability is analytically known [21, 22]. A critical b_0 of the order of 300 has been found.

In contrast to the *ab initio* theoretical approach of [21], we present here an experimental evaluation of the threshold of a random laser. Our method relies on the fact that thanks to Kramers-Kronig relations [23], the complex atomic polarizability is indeed one *single* independent parameter, and thus can be fully determined by a spectroscopic measurement. This idea is general and could be applied with any gain mechanisms. We demonstrate its usefulness here with Raman gain between non-degenerate Zeeman states [18, 19, 24, 25]. We obtain a critical optical thickness on the order of 200, lower than with Mollow gain [21].

2. Measuring the threshold of a random laser with cold atoms

From Letokhov's diffusive description of light transport in a homogeneous, disordered and active medium of size L , we know that the random laser threshold is governed by two characteristic lengths: the elastic scattering mean free path ℓ_{sc} [26, 27] and the linear gain length ℓ_g ($\ell_g < 0$ corresponds to absorption or inelastic scattering). In the diffusive regime, defined as $L \gg \ell_{sc}$, the lasing threshold is reached when the unfolded path length, on the order of L^2/ℓ_{sc} , becomes larger than the gain length. More precisely, the threshold is given by [1, 13]

$$L_{\text{eff}} > \beta \pi \sqrt{\ell_{sc} \ell_g / 3}, \quad (1)$$

where β is a numerical factor that depends on the geometry of the sample ($\beta = 1$ for a slab, $\beta = 2$ for a sphere, which is the case we consider in the following), and $L_{\text{eff}} = \eta L$ is the effective length of the sample, taking into account the extrapolation length [26]. For $L > \ell_{sc}$ and a sphere geometry, $\eta = 1 + 2\xi / [L/\ell_{sc} + 2\xi]$ with $\xi \simeq 0.71$ [28, 29]. Note that deeply in the diffusive regime ($L \gg \ell_{sc}$), $\eta \sim 1$. Another important length scale is the extinction length ℓ_{ex} , as measured by the forward transmission of a beam through the sample, $T = e^{-L/\ell_{\text{ex}}}$. The extinction length is related to the other lengths by $\ell_{\text{ex}}^{-1} = \ell_{sc}^{-1} - \ell_g^{-1}$.

For an atomic vapor, these characteristic lengths can both be computed as a function of the atomic polarizability $\alpha(\omega)$ at frequency ω . The extinction cross-section is indeed given by $\sigma_{\text{ex}}(\omega) = k \times \text{Im}[\alpha(\omega)]$ and the elastic scattering cross-section by $\sigma_{sc}(\omega) = k^4 / 6\pi \times |\alpha(\omega)|^2$

[30] ($k = \omega/c$ is the wave vector). Note that the first relation is general to any dielectric medium whereas the second one is specific to resonant point-dipole scatterers. The characteristic lengths are then $\ell_{\text{ex,sc}}^{-1} = \rho \sigma_{\text{ex,sc}}$, where ρ is the atomic density. The gain cross-section can be defined the same way by $\ell_{\text{g}}^{-1} = \rho \sigma_{\text{g}}$. The vapor is supposed homogeneous, as well as the pumping field, so that both ρ and α are position-independent. Even though this is not the precise geometry of a cold-atom experiment, it allows us to perform analytical estimations. As we consider only quasi-resonant light, we shall use $k = k_0 = \omega_0/c$ with ω_0 the atomic eigenfrequency. In the following, we shall also use a dimensionless atomic polarizability $\tilde{\alpha}$, defined as $\alpha = \tilde{\alpha} \times 6\pi/k_0^3$, and omit the dependence on ω . We can now rewrite $\sigma_{\text{sc}} = \sigma_0 |\tilde{\alpha}|^2$ and $\sigma_{\text{g}} = \sigma_0 (|\tilde{\alpha}|^2 - \text{Im}(\tilde{\alpha}))$, where $\sigma_0 = 6\pi/k_0^2$ is the resonant scattering cross-section, such that the threshold condition, as expressed by Eq. (1), reduces to

$$\rho \sigma_0 L_{\text{eff}} = \eta b_0 > \frac{2\pi}{\sqrt{3} |\tilde{\alpha}|^2 (|\tilde{\alpha}|^2 - \text{Im}(\tilde{\alpha}))}, \quad (2)$$

where b_0 is the on-resonance optical thickness of the cloud. This condition is valid as soon as the medium exhibits gain, *i.e.* $|\tilde{\alpha}|^2 - \text{Im}(\tilde{\alpha}) > 0$.

The threshold condition is thus given by a critical on-resonance optical thickness, which is an intrinsic parameter of the cloud, expressed as a function of the complex atomic polarizability only, which depends on the pumping parameters. Although the initial condition of Eq. (1) involves two characteristic lengths, we emphasize here that this is really one single independent parameter, as real and imaginary parts of the atomic polarizability are related via Kramers-Kronig relations [23]. This point is due to the originality of the system that we are considering, in which the same atoms are used to amplify and scatter light.

This property has two important practical consequences. The first one is that we cannot adjust one quantity (for example gain) independently of the other (scattering rate, or vice versa), so that the existence of reasonable conditions for random lasing is not obvious. This issue has been positively answered recently and it has been shown that random lasing can even occur with a low amount of scattering [21]. The second one is that only one quantity has to be measured to determine the threshold, as soon as we can measure it for every ω , since Kramers-Kronig relations involve integrals over ω . A weak probe transmission spectrum, which we can rewrite, with our notations, $T(\omega) = \exp[-b_0 \times \text{Im}(\tilde{\alpha}(\omega))]$, contains therefore enough information to fully characterize $\tilde{\alpha}(\omega)$ and then to deduce the critical optical thickness. In the following, we use this idea with Raman gain.

Note that without this possibility, measuring independently the two characteristic lengths is difficult. Besides the transmission spectrum, one needs another measurement, which can be provided by the fluorescence. Nevertheless, the probe fluorescence is small compared to the pump one, and inelastic scattering is not easily distinguished from elastic scattering. Despite these difficulties, preliminary measurements, in a limited range of parameters, have qualitatively validated the approach based on Kramers-Kronig relations [31].

3. Application to Raman gain

Our experiment uses a cloud of cold ^{85}Rb atoms confined in a vapor-loaded magneto-optical trap (MOT) [15] produced by six large independent trapping beams, allowing the trapping of a few 10^9 atoms at a density of 10^{10} atoms/cm³, corresponding to an on-resonance optical thickness of about 10. To add gain to our system, we use a pump beam, which is tuned near the $F = 3 \rightarrow F' = 4$ cycling transition of the $D2$ line of ^{85}Rb (frequency ω_0 , wavelength $\lambda = 780$ nm, natural linewidth $\Gamma/2\pi = 6.1$ MHz), with a detuning $\Delta = \omega_{\text{p}} - \omega_0$, which can be changed via an acousto-optic modulator in a double-pass configuration. The pump beam has a linear polarization and a waist larger than the MOT size (a few millimeters) to ensures

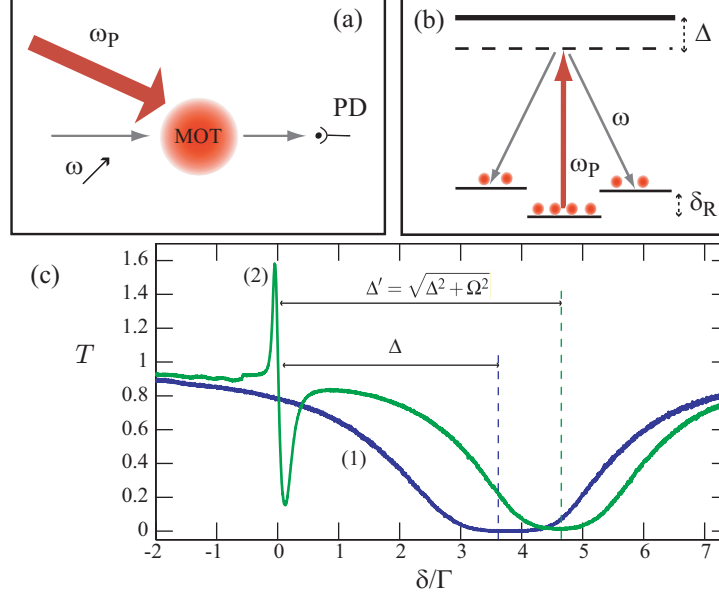


Fig. 1. (a) Principle of the experiment. We send a weak probe beam on the magneto-optical trap (MOT) and the transmission is recorded on a photodetector (PD). The probe frequency ω is ramped during the acquisition in order to record a spectrum. Another, stronger beam of frequency ω_P is used as a pump. (b) Principle of the Raman mechanism (depicted here for a $F = 1 \rightarrow F' = 2$ transition). (c) Experimental transmission spectra, plotted as a function of the pump-probe detuning δ . Without pumping, spectrum (1) shows only the atomic absorption. A pump beam of detuning $\Delta = -3.8\Gamma$ and intensity 13 mW/cm^2 , corresponding to a Rabi frequency $\Omega = 2.5\Gamma$, is added to obtain spectrum (2), which then exhibits a Raman resonance in the vicinity of $\delta = 0$. The atomic absorption is shifted due to the pump-induced light shift and the absorption is reduced due to saturation.

homogeneous pumping. An additional, orthogonally polarized beam is used as a weak probe to measure transmission spectra with a propagation axis making an angle with the pump-beam axis of about 17° [Fig. 1(a)]. This small angle, together with the low temperature of our sample ($\sim 100 \mu\text{K}$) allows us to neglect any relative Doppler broadening ($\sim 40 \text{ kHz}$). The probe frequency ω can be swept around the pump frequency with a detuning $\delta = \omega - \omega_P$. Both lasers, pump and probe, are obtained by injection-locking of semiconductor lasers from a common master laser, which allows to resolve narrow spectral features (this has been checked for earlier experiments [19] down to 10 kHz). All our experiments are time-pulsed with a cycling time of 30 ms . The trapping period lasts 29 ms , followed by a dark period of 1 ms , when the MOT trapping beams and magnetic field are switched off. In order to avoid optical pumping into the dark hyperfine $F = 2$ ground state, a repumping laser is kept on all time. Pump-probe spectroscopy is performed during the dark phase, short enough to avoid expansion of the atomic cloud. Data acquisitions are the result of an average of 300 cycles.

Raman gain relies on the pump-induced population inversion among the different light-shifted m_F Zeeman sublevels of the $F = 3$ hyperfine level [24, 25], as depicted in Fig. 1(b). The optical pumping induced by the π -polarized pump laser leads to a symmetric distribution of population with respect to the $m_F = 0$ sublevel of the ground state, with this sublevel being the most populated and also the most shifted, due to a larger Clebsch-Gordan coefficient [32]. Atoms are probed with a π -polarized (with perpendicular direction) probe beam, thus inducing

$\Delta m_F = \pm 1$ Raman transitions. Depending on the sign of the pump-probe detuning δ , the population imbalance induces gain or absorption. Each pair of neighboring sublevels contributes with a relative weight depending on the population inversion. In practice however, the levels are not separated enough to be well resolved, and only two structures (with opposite signs) are visible, one corresponding to amplification for $\delta = -\delta_R$ and one to absorption for $\delta = \delta_R$. Note that this situation corresponds to a red detuning for the pump ($\Delta < 0$) and that the signs are inverted for blue-detuning ($\Delta > 0$). As δ_R comes from a differential light-shift (because of different Clebsch-Gordan coefficients), it is usually on the order of $\Gamma/10$, whereas Δ is a few Γ . The width γ of the resonances is related to the elastic scattering rate, also much smaller than Γ [24]. Far from the main atomic absorption resonance, the Raman resonance is thus a narrow spectral feature, as in Fig. 1(c), such that we can fit it independently of the main absorption line [Fig. 2(a)]. Therefore, we scan the frequency of the probe beam around $\delta = 0$ only, which reduces the interaction time with the pump, thus suppressing radiation pressure and subsequent unwanted Doppler shift. Note that adding a second counterpropagating pump beam is not a suitable solution, as in this situation, other mechanisms may occur (recoil-induced resonances, four-wave mixing, atom localization in potential wells) [32, 33, 34], which would complicate the analysis. We use the polarizability $\tilde{\alpha}_R(\delta, \Delta, \Omega)$ to describe the Raman structure, with

$$\text{Im}(\tilde{\alpha}_R) = \frac{A_1}{(\delta - \delta_R)^2 + \gamma^2/4} - \frac{A_2}{(\delta + \delta_R)^2 + \gamma^2/4}. \quad (3)$$

This function is particularly convenient as the Kramers-Kronig transformation of a Lorentzian profile is well known. We thus avoid any numerical integration.

Our experimental procedure is the following. We scan the probe frequency from $\delta = -\Gamma$ to $\delta = \Gamma$ during $100 \mu\text{s}$ and record one Raman transmission spectrum. During the same cycle, we perform two larger scans without pumping, one before the pump-probe spectroscopy and one after, in order to record the main absorption line (as in Fig. 1(c)), from which we extract the on-resonance optical thickness b_0 . The second measurement allows us to take into account the losses induced by the pump radiation pressure. The corresponding uncertainty on b_0 induces, at the end, a $\pm 10\%$ uncertainty on the critical optical thickness. Then, we fit by

$$T(\delta) = \exp[-b_0 \times (\text{Im}[\tilde{\alpha}_R(\delta)] + m\delta + p)], \quad (4)$$

where A_1 , A_2 , δ_R and γ are the adjustable parameters of the Raman structure described by $\tilde{\alpha}_R$, and the adjustable line parameterized by m, p is used to fit the background of the transmission spectrum. This expression is not rigorous and one could instead search for the complete expression of the atomic response. However, it is difficult to take into account the complete real system, including the Zeeman degeneracy and polarization effects. Using Eq. (4) allows us to efficiently measure the Raman parameters. As shown in Fig. 2(a), the fit is very satisfactory. For most parameters, the width γ of the Lorentzians is larger than their shift δ_R , so that the two Lorentzians are not separated and the Raman structure looks like a dispersion profile. Similarly, the corresponding scattering cross-section looks like one bell-shaped curve. The obtained widths γ are consistent with the pump elastic scattering rate. The ratio between the gain amplitude A_1 and the absorption amplitude A_2 is approximately constant, as expected, since it depends only on the Clebsch-Gordan coefficients.

Then, the Lorentzian shape of the Raman contribution to the atomic polarizability is analytically transformed through Kramers-Kronig relations to get

$$\text{Re}(\tilde{\alpha}_R) = A_1 \times \frac{-2(\delta - \delta_R)/\gamma}{(\delta - \delta_R)^2 + \gamma^2/4} - A_2 \times \frac{-2(\delta + \delta_R)/\gamma}{(\delta + \delta_R)^2 + \gamma^2/4}. \quad (5)$$

The atomic polarizability $\tilde{\alpha}_R$ is thus fully determined.

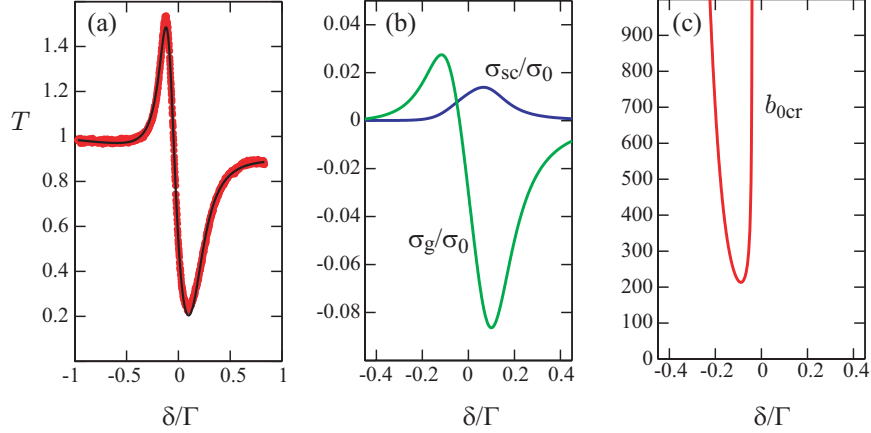


Fig. 2. (a) Typical experimental spectrum (red dots) and its fit (black line) around the Raman resonance. The parameters obtained from the fit are $A_1 = 0.21$ (gain amplitude), $A_2 = 0.11$ (absorption amplitude), $\gamma = 0.25\Gamma = 1.5$ MHz and $\delta_R = 0.09\Gamma = 540$ kHz. (b) Gain and scattering cross sections, computed from Eqs. (6,7) with the Raman parameters deduced from the fit. (c) Corresponding critical optical thickness. The minimum is $b_0 \simeq 220$. This set of data corresponds to the pump parameters $\Delta = -3.4\Gamma$ and $\Omega = 3.4\Gamma$.

However, the measurement is valid for the special polarization configuration that we have used, whereas for a random laser, the polarization is *a priori* random. To get a realistic estimation of the random laser threshold, we thus have to make an average over the polarization. We have checked experimentally that the coefficients A_1 , A_2 have a $\sin^2(\theta)$ dependence with the relative angle θ between the pump and the probe linear polarizations. As we have performed all the measurements in the optimum case (with the probe polarization perpendicular to the pump one), it is appropriate to multiply the measured values of $\text{Im}(\tilde{\alpha}_R)$ by $1/2$ and $|\tilde{\alpha}_R|^2$ by $3/8$ (average of $\sin^4(\theta)$). The cross-sections used to determine the random laser threshold are thus

$$\sigma_g/\sigma_0 = \frac{3}{8}|\tilde{\alpha}_R|^2 - \frac{1}{2}\text{Im}(\tilde{\alpha}_R), \quad (6)$$

$$\sigma_{sc}/\sigma_0 = \frac{3}{8}|\tilde{\alpha}_R|^2, \quad (7)$$

where $\tilde{\alpha}_R$ is experimentally determined as described above [Eqs. (3-5) and Fig. 2(a)]. An example of computed cross-sections is shown in Fig. 2(b).

Then, the critical optical thickness is easily computed from

$$\eta b_{0cr} = \frac{2\pi\sigma_0}{\sqrt{3\sigma_{sc}\sigma_g}}, \quad (8)$$

where the correcting η factor (coming from the extrapolation length) writes $\eta = (b_{0cr}\sigma_{sc} + 4\zeta\sigma_0)/(b_{0cr}\sigma_{sc} + 2\zeta\sigma_0)$ and yields a second-order equation in b_{0cr} . The solution, plotted as a function of δ , is reported on Fig. 2(c). As expected, the minimum is located near the maximum of the gain cross-section, *i.e.* for $\delta \simeq -\delta_R$.

4. Results and discussion

We repeat the above procedure for each couple of pumping parameters $\{\Delta, \Omega\}$. The Rabi frequency of the atom-pump interaction has been calibrated by monitoring the light shift of the

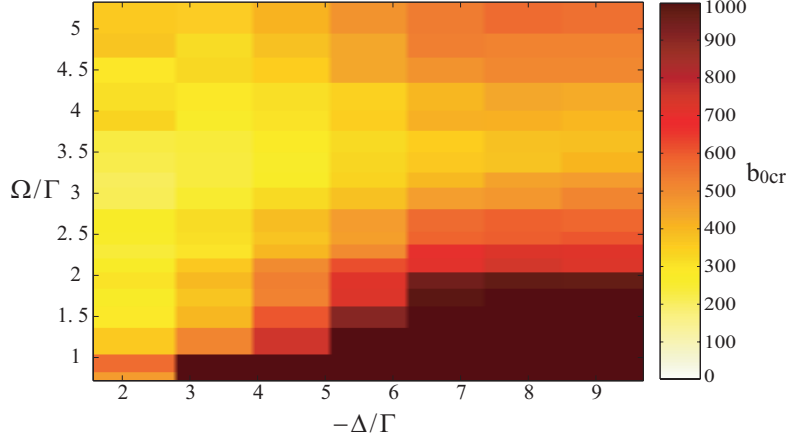


Fig. 3. Critical optical thickness b_{0cr} as a function of the pumping parameters Δ (atom-pump detuning) and Ω (Rabi frequency of the atom-pump coupling). The minimum is around $b_{0cr} \sim 210 - 230$, for $\Delta \sim 2\Gamma$ and $\Omega \sim 2 - 3\Gamma$.

main absorption line [35] as a function of the pump intensity, as it can be seen in Fig. 1(c). We studied only the $\Delta < 0$ part, as Raman gain is independent on the sign of Δ [34]. Moreover, we have been restricted to $|\Delta| \geq 2$ because too much radiation pressure destroys the MOT for $|\Delta| < 2$. As the random laser will automatically start with the first frequency above threshold, we report in Fig. 3 the critical optical thickness defined as

$$b_{0cr}(\Delta, \Omega) = \min_{\delta} [b_{0cr}(\delta, \Delta, \Omega)]. \quad (9)$$

The minimum is around $b_{0cr} \sim 210 - 230$, obtained for $\Delta \sim 2\Gamma$ and $\Omega \sim 2 - 3\Gamma$.

Once the critical optical thickness is computed, the self-consistency of our model has to be checked on two points. Firstly, the diffusive approach leading to Eq. (1) requires in principle that the ratio $L/\ell_{sc} = b_{0cr} \times \sigma_{sc}/\sigma_0$ is substantially larger than one to be justified. Nevertheless, it has been shown recently that this condition has not to be strictly respected, as the diffusive approach gives quite accurate results down to $L/\ell_{sc} \sim 1$ [21]. This is approximately the value obtained for the optimum parameters. Note also that the correction due to the extrapolation length (η factor) is not negligible, as for $L/\ell_{sc} \sim 1$, $\eta \sim 1.6$.

Secondly, we have so far only considered the Raman resonance, neglecting the influence of the main atomic transition at ω_0 , which is valid for very large detunings $\Delta \gg \Gamma$. However, since the optimum threshold is obtained for small detuning, this is not justified. The corresponding one-photon transition has no gain around $\delta = 0$ and then only adds scattering. This scattering can be decomposed into elastic and inelastic contributions. The elastic contribution will lower the random laser threshold, whereas the inelastic contribution, which shifts the frequency out of the Raman gain curve, will yield an increase of the lasing threshold. Let us examine the effect of the supplementary elastic scattering. It can be evaluated by

$$\sigma_{el} = \frac{\sigma_0}{1 + 4\Delta^2/\Gamma^2} \times \frac{1}{(1+s)^2} \times \mathcal{C}. \quad (10)$$

The first term is the total scattering cross-section of a two-level atom, taking into account the detuning. The second factor, where $s = 2\Omega^2/(\Gamma^2 + 4\Delta^2)$ is the pump saturation parameter, describes the reduced scattering cross-section, keeping only the elastic part [35]. As a change of Zeeman sublevel is possible during a scattering event, an additional weighting factor, estimated

as $\mathcal{C} \sim 0.5$ [36], is necessary to select true elastic scattering. Adding σ_{el} to σ_{sc} [Eq. (7)] lowers the critical optical thickness to $b_{0\text{cr}} \sim 120 - 130$, with approximately the same optimum pumping parameters. This is however an optimistic evaluation, as inelastic scattering has not been taken into account. On the contrary, a conservative evaluation can be obtained by considering inelastic scattering as pure losses, *i.e.* as a negative contribution to the gain cross-section. This is pessimistic because those photons may not be definitively lost, as further inelastic scattering can shift their frequency back on the gain curve. As previously, the inelastic scattering cross-section can be evaluated by

$$\sigma_{\text{inel}} = \frac{\sigma_0}{1 + 4\Delta^2/\Gamma^2} \times \left[\frac{1}{(1+s)^2} \times (1 - \mathcal{C}) + \frac{s}{(1+s)^2} \right]. \quad (11)$$

The first term in the squared bracket is associated with Raman inelastic scattering whereas the second term is due to incoherent scattering of the two-level atom [37]. Subtracting σ_{inel} to the gain cross-section of Eq. (6) increases now the critical optical thickness to $b_{0\text{cr}} \sim 215 - 230$. The optimum parameters are then located near $\Omega \sim 3 - 4\Gamma$ and $\Delta \sim 3 - 4\Gamma$. Except for small Δ , where inelastic scattering is dramatic, the result is not very different from the one presented on Fig. 3. Especially near the optimum parameters ($\Omega = \Delta \sim 3 - 4\Gamma$), the optimistic evaluation leads to $b_{0\text{cr}} \sim 165 - 180$, which is not very different from the pessimistic result ($b_{0\text{cr}} \sim 215 - 230$). Therefore, we conclude that the value $b_{0\text{cr}} \sim 200$ gives the correct order of magnitude. Such a high optical thickness is achievable, for instance by using compression techniques of magneto-optical traps [38, 39]. The corresponding ratio L/ℓ_{sc} is on the order of 2.

Random lasing occurs at a detuning from the pump $|\delta| \sim \delta_{\text{R}}$, typically smaller than 1 MHz. This makes the detection of such a random laser very challenging, as the corresponding fluorescence cannot easily be separated from the pump-induced fluorescence. Nevertheless, the narrow Raman structure could be revealed by a beat note experiment, as in [40], or alternatively by the intensity correlations in the fluorescence, measured either by a homodyne technique [41] or with a time correlator [42]. In this last experiment, a contribution from Raman scattering has been measured, consistent with the theoretical predictions of [36]. It seems reasonable to expect this signal to have different behaviors below and above threshold, but this remains to be checked by further theoretical studies.

Finally, let us mention that our model contains several limitations, so that the numbers should be considered as first-order estimates. Our description of Raman gain is quite simplified in order to have an efficient data analysis procedure, leading to quasi-analytical results. Precise modelling of the complete atomic response is indeed not the goal of this article. On the contrary, Raman gain is used as a convenient example to illustrate the method, which is general and could be used with any gain mechanism, by numerically computing the real part of the atomic polarizability from the experimental transmission spectrum, via Kramers-Kronig relations.

Our hypothesis of homogeneous atomic density and monochromatic and homogeneous pumping could also be discussed [43], especially when high optical thicknesses are involved, as the pump attenuation may become important. These effects could be taken into account in numerical simulations of light transport in active and disordered medium, but have to be neglected to allow the analytical resolution of the diffusion equation leading to Eq. (1) [1, 13]. Note however that the on-resonance optical thickness is not the relevant parameter for the pumping field, since the pump is detuned and is saturating. Moreover, diffused pump light, which penetrates into the sample much deeper than the coherent transmission, has also to be taken into account.

5. Conclusion

We have presented a method to experimentally determine the threshold of random lasing in a cloud of cold atoms. In this specific system, the threshold is related only to the complex atomic

polarizability, which can be fully characterized by spectroscopic measurements. We applied this idea with Raman gain between light-shifted Zeeman sublevels of rubidium atoms. From our measurements, we estimate the critical optical thickness to be on the order of 200, which is achievable with current cold-atom experiments.

The obtained critical optical thickness is lower than the one obtained with Mollow gain [21]. This is in agreement with the intuition that more complex gain mechanisms offer more degrees of freedom, which is of course necessary to optimize several quantities (scattering and gain) at the same time. We are then confident that even lower thresholds can be obtained with other, more complex gain mechanisms, for example non-linear parametric gain induced by non-degenerate four-wave mixing. This may be the subject of our future investigations.

Acknowledgments

We thank F. Michaud and R. Carminati for fruitful discussions. We acknowledge financial support from the program ANR-06-BLAN-0096, funding for N.M. by DGA and for D.B. by INTERCAN.